GEOLOGY

ADIL A. ALIYEV, ORHAN R. ABBASOV

Institute of Geology and Geophysics, Azerbaijan National of Academy Sciences, 119, H. Javid ave., Baku, AZ1143, Azerbaijan, tel.: (+99412) 5100141, e-mail: ad_aliyev@mail.ru, ortal80@bk.ru

NATURE OF THE PROVENANCE AND TECTONIC SETTING OF OIL SHALE (MIDDLE EOCENE) IN THE GREATER CAUCASUS SOUTHEASTERN PLUNGE

Objective. The protolith and tectonic settings of the Middle Eocene oil shale sampled from the outcrops and ejected products of mud volcanoes in the Greater Caucasus southeastern plunge were determined using bulk rock geochemistry data. The obtained results were adapted to the palaeogeodynamic conditions of the study areas. **Method.** The concentrations of element content in the samples were measured by "S8 TIGER Series 2 WDXRF" and "Agilent 7700 Series ICP-MS" mass spectrometers. The microscopes "Loupe Zoom Paralux XTL 745" and "MC-10" and a digital camera "OptixCam" were used to define the age of samples. The distribution of element contents of samples was normalized to Post-Archaean Australian shale (PAAS), Upper Continental Crust (UCC) and Continental Crust (CC). The source terrains of the parent rocks and tectonic settings of oil shale were determined using various ratios and diagrams. **Results.** The samples show a nature of basaltic and basalt andesitic protolith, which supports an idea that the original composition was derived from mafic and intermediate source terrains. The tectonic setting of oil shale correlates well with the active continental margin and the rift-to-collision transition or paleogeodynamic conditions of the initial collision. Thus, in the shallow sea basin and the initial collision conditions, the process of sedimentation in the middle Eocene was probably associated with the final Paleocene-Eocene basin, which was the northern branch of Meso-Tethys in the Crimea-Greater Caucasus-Kopetdag system. The Jurassic and Cretaceous volcanism associated with subductions, which occurred on the southern slope of the Greater Caucasus (in the Tufan and Vandam uplifts), played an important role as a source of transported materials. **Scientific novelty.** In the published literature, numerous geological and organic-geochemical features of oil shale in Azerbaijan have been studied. The literature on the study of the provenance and tectonic setting is nonexistent, and this study is the first attempt. Practical significance. The obtained results and the used methodology can be applied to study the genesis of the Middle Eocene deposits and as well as sedimentary rocks in Azerbaijan.

Key words: Great Caucasus; oil shale; bulk rock geochemistry; protolith; tectonics; geodynamics; volcanism; basin

Introduction

The Shamakhi-Gobustan region and Absheron Peninsula are the southeastern plunges of the Greater Caucasus (Fig. 1, *a*) located in the collision zone between the Arabian and the Eurasian continents. A very high sedimentation rate is characteristic for Eastern Azerbaijan. Such specific geodynamic and paleogeographic conditions are favorable for the formation of hydrocarbons, mud volcanoes, and especially oil shale in these areas.
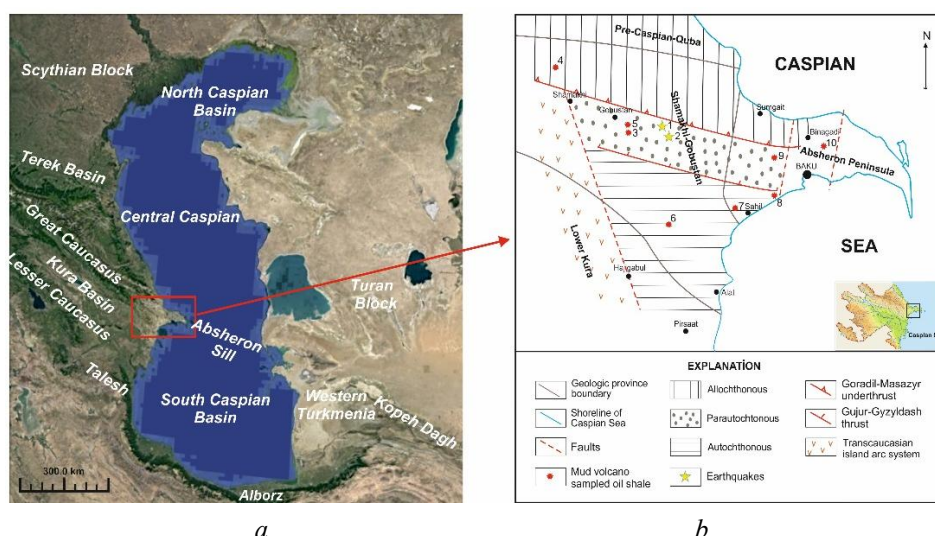

a   *b*

Fig. 1. Location map of oil shale samples taken from outcrops and mud volcanic areas

Azerbaijan is one of the oldest and richest oil and gas countries in the world. The largest and long-known oil and gas fields onshore and in the Caspian Sea led to a weak study of unconventional hydrocarbon resources in the Republic, in particular, oil shale. However, oil shale as a secondary fuel and energy resources have great potential in Azerbaijan (Abbasov et al., 2013; Aliyev et al., 2015; Aliyev & Abbasov, 2016). Forecast sources of oil shale in the country are estimated at 500 million tons (Abbasov, 2015). In addition, based on a comparative analysis, it was determined that the main qualitative parameters (organic matter (15–31 %), sulfur (0.4–1.2 %), ash content (65–85 %) and calorific value (6.0–12 MJ/kg)) of the oil shale deposits such as Guba, Diyally, Jangichay, Kichik Siyeki and others in Azerbaijan exceed low-calorie deposits of oil shale in a number of countries, like Germany, Romania, China, etc. (Abbasov, 2015; Aliyev et al., 2015; Aliyev & Abbasov, 2016).

Oil shale of the republic has great potential as a source rock (Abbasov et al, 2015). The oil shale layers in Central Gobustan, which were studied at relatively shallow depths, are considered as a future source of shale gas for the country (Abbasov, 2016) .

Overall, in Azerbaijan, about 60 outcrops of oil shale were recorded (Aliyev et al., 2014; Aliyev et al., 2015). Most of the outcrops are characterized by a large thickness and wide spatial distribution belonging to the Middle Eocene (Abbasov, 2009).

Along with outcrops, oil shale is also found in the ejected products of the mud volcanoes of the study areas (Aliyev and Abbasov, 2018). In these rocks, the *Globigerina bulloides (Orbigny), Cibicides sp., Globigerina triloculinoides (Plummer)*, benthos and planktonic foraminifera, as well as fish teeth and bones were encountered, which conencide to the Middle Eocene.

In the published literature, the geological characteristics, organic geochemical properties, probable resources, and prospects for the use of oil shale in Azerbaijan have been studied (Abbasov, 2009; Abbasov et al., 2013; Aliyev et al., 2014; Abbasov, 2016; Abbasov, 2017; Aliyev and Abbasov, 2018; Aliyev et al., 2018). However, a study on the genesis, especially implications for provenance and tectonic setting is not found in the published literature. In this regard, this research is dedicated to the reconstruction of the origin of oil shale, as well as palaeotectonic conditions in the Middle Eocene in the study areas.

Geological and geotectonical background

Shamakhi-Gobustan region. In the region, about 40 outcrops of oil shale were recorded (Abbasov, 2009; Aliyev et al., 2014). The geological structure of the region consists of Mezo-Cenozoic sediments. The rocks contained oil shale are associated with the sediments of the Cretaceous-Upper Miocene (Aliyev and Abbasov, 2018).

The Upper Cretaceous sediments were found in the northern part of the region, which mainly consists of alternating layers of mudstone, marl and limestone. The thickness of the oil shale layers found in such a mixed litofacial section is small, and they contain less organic matter (Abbasov et al., 2013).

The variability of the thickness and instability of the lithofacies of the Middle Eocene is characteristic of the region. The basis of lithofacies is made up of light shale and layers of light brown oil shale. The thickness of the layers of oil shale found on the wings and ridges of anticlines and synclines, such as Kichik Siyeki, Jangichay, Jangidagh vary from a few centimeters to about 10 meters. (Abbasov, 2009). The sections of Jangichay and Kichik Siyeki located in the central part of the region and are included in the current study. Both sections were studied in detail.

Laying of oil shale beds is similar to the arch line of the Jangichay anticline. These beds are followed by the valley of the Jangichay River in the eastern part of Central Gobustan. The oil shale beds have been identified on both wings of the anticline. Layers containing black and black-gray oil shales lie in over 3 km. The average thickness of the studied section is about 200 m. In the investigated section, the oil shale layers are mainly replaced by mudstone. Thin layers of sandstone and dolomite were also recorded in the section (Fig. 2).

Layers of oil shale are observed along the southeastern pericline of the Kichik Siyeki syncline on an area of over 2.5 km. The total thickness of the studied section is more than 270 meters. As in Jangichay, depending on the depth, an increase in the number and thickness of the oil shale layers is recorded. The section mainly consists of alternating layers of oil shale and mudstone. Dolomite and limestone are characteristic of the upper part of the section (Fig. 2). The studied samples were taken from the upper part of both sections.

The upper Maikopian sediments are divided into two lithofacies, which differ sharply from one another: northern mudstones and southern sandy-mudstone. In areas where both lithofacies spread, three horizons are divided: Riki, Siderit and Sideritustu. The layers of oil shale are associated with the lower part of the Upper Maikopian sediments, which corresponds to the Riki horizon. In the Khilmilly outcrop and in a syncline located between the Goradil and Tuva uplifts, the thickness of the shale layers increases from 0.5 to 5 m.

The sediments of the Konkian horizon mainly consist of light-gray, brown-gray mudstones and carbonate rocks. In the central, northwest and southwest of Gobustan, such lithofacies replace with the layers of oil shale.

The upper Sarmatian section is characterized by unstable lithofacies in the Northern Gobustan. The lower part of the section is rich in gray mudstone. Sandstone and sandy-clay rocks are recorded in the middle part of the section. Volcanic ash is observed at the top. In the center of Gobustan, in the wings of large anticlines and on the slopes between them, the oil shale beds are traced.
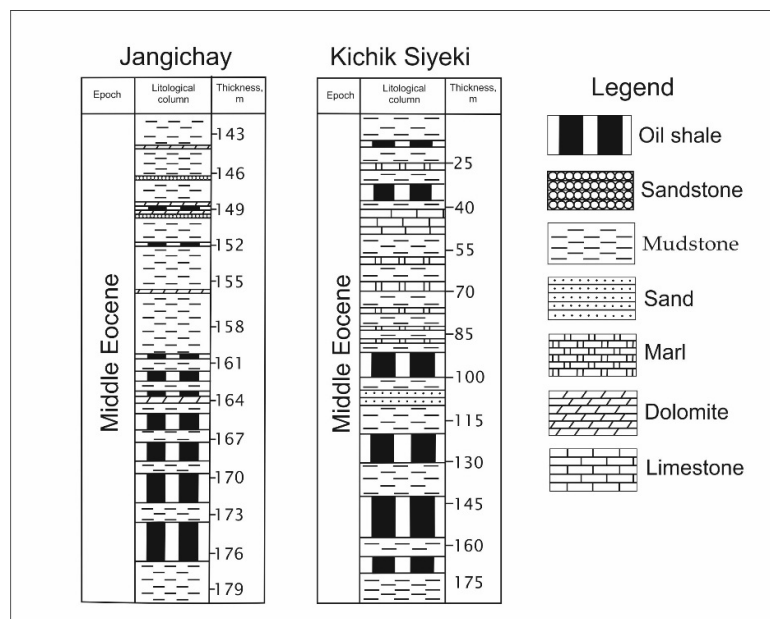
Fig. 2. Stratigraphic columns of the studied sections of oil shale outcrops
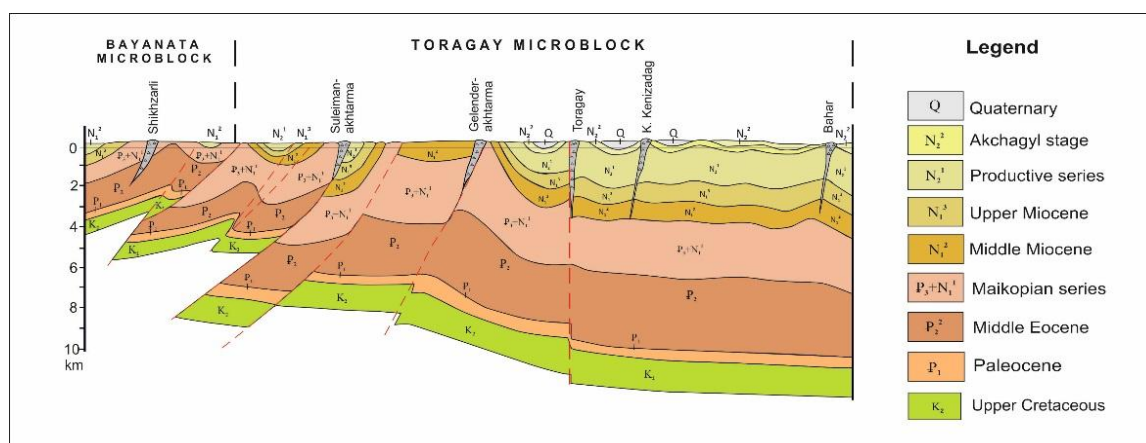

Fig. 3. Geological profile of Bayanata and Toragay microblocks (after Aliyev et al., 2015)

Due to the nature of neotectonics, a thrust zone (allochthonous) has been identified between the Gujur-Gyzyldash thrust and the Goradil-Masazir underthrust that is called the North Gobustan (Fig. 1, b). In allochthonous, the flyshoids of the Cretaceous (Baskal overthrust mass) cover the Paleogene-Miocene sediments. The Bayanata microblock (parautochtonous) is located in the south of the Goradil-Masazir underthrust and limited by the Gujur-Gyzyldash thrust (Fig. 1, b). The thickness of the Paleogene-Miocene sediments in this microblock is 2.5–4.5 km (Fig. 3). This zone of the Central Gobustan is the most widespread area for exposure (Boyuk and Kichik Siyeki, Jangichay, etc.) of the Middle Eocene oil shale in the Shamakhi-Gobustan region (Abbasov, 2009).

The geological structure of the Toragay microblock (autochthonous) consists of the Cenozoic sediments. The top of the Upper Cretaceous lies at a depth of 8–11.5 km (Fig. 3).

In general, the Middle Eocene sediments are very important for the Shamakhi-Gobustan region in terms of oil shale lithofacies. Besides with the outcrops, the determined geological age (Middle Eocene) of oil shale sampled from the mud volcanoes (Shikhzarli, Demirchi, Bozaakhktarma and Qotur) significantly increases this conviction. The thickness of Middle Eocene sediments varies from approximately 1.7 km (Central Gobustan) to 3.8 km (Southern Gobustan). See Fig. 3. **Absheron Peninsula.** 18 outcrops of oil shale were revealed here (Aliyev et al., 2014). The geological structure of the region consists of terrigenous and carbonate rocks of the Upper Cretaceous-Cenozoic.

The Eocene oil shale is found only in the folded areas of Goytepe and Govundagh. Oil shale outcrops of the Peninsula are mainly associated with the Upper Maikopian Series and Upper Miocene (Aliyev et al., 2014; Abbasov, 2017).

Black oil shale beds, associated with the Maikopian series, were found on the northern slope of the Uchtepe-Shorchala mountains, on a 112-meter section of the Riki horizon in Goytepe, Orjandagh and Fatmayi.

In the Konkian section, associated with terrigenous and carbonate rocks, layers of bituminous oil shale (total thickness 30 m) were found in the Shorbulag and Qaraheybet regions of the Western Absheron. Laminated layers of oil shale are also traced in the folds of Uchtepe-Ilkhydagh, Goytepe, Kechaldagh-Zigilpiri, as well as in the north of the Kecheldagh mud volcano, and in the west of the Binagadi settlements. The layers of oil shale found in the outcrops are mostly black.

Oil shale associated with the Meotian on the peninsula is recorded in the Shorbulag region, located in the Western Absheron, as well as on the Kusmelidagh and Uchtepa synclines. Beds of oil shale are also found in Ateshgah, Khirdalan, Shabandagh, Binagadi and other areas. Their thickness is 4.5 m, and the length is more than 1.5 km.

The region is the end of the south-eastern plunge of the Greater Caucasus due to its tectonic and spatial position. Most of the tectonic zones studied here incline from the north-west to the south-east, in the direction of the extension of the Greater Caucasus, and gradually deepen in the south-east. The Mesozoic complex in the south of the Absheron Peninsula abruptly descends. The Paleogene-Pliocene sediments dominate in the geological structure of the uplift, that some outcrops of oil shale (Khirdalan, Zigilpiri, etc.) are associated.

Four tectonic zones have been defined on the peninsula, and there is a morphological link between the anticlinals and the synclines. Due to tectonic nature, the peninsula is subject to dislocations and complicated with mud volcanoes Keyreki, Lokbatan, Bozdagh-Qobu, etc. (Aliyev et al., 2015).

Objective

The protolith and palaeotectonic settings of samples were taken from the outcrops and ejected materials of mud volcanoes in Shamakhi-Gobustan region and on the Absheron peninsula located in the Greater Caucasus southeastern plunge, were defined based on evidence from geochemistry of oil shale, and the results were adapted to the palaeogeodynamic evolution characteristics of the study area in the Middle Eosene.

Methodology

Samples: two samples from the outcrops (1 – Kichik Siyaki, 2 – Jangichay) and eight samples from ejected materials of mud volcanoes (3 – Shikhzarli, 4 – Demirchi, 5 – Bozaakhtarma, 6 – Qotur, 7 – Otmanbozdagh, 8 – Lokbatan, 9 – Bozdagh-Qobu, 10 – Keyreki) were taken (Fig. 1b). The samples are black, gray and brown in color with a laminated structure.

Bulk rock geochemistry: analysis of major and trace elements were performed on the "S8 TIGER Series 2 WDXRF" and "Agilent 7700 Series ICP-MS" using mass spectrometers at the Institute of Geology and Geophysics, Azerbaijan National Academy of Sciences.

Age of rocks: ages of samples taken from the mud volcanic areas were determined using microscopes "Loupe Zoom Paralux XTL 745" and "МБС-10" and a digital camera "OptixCam" at the Integrated Engineering Exploration Production, Department of Geophysics and Geology, SOCAR.

The distribution of element contents of samples normalized to PAAS (Taylor and McLennan, 1985), UCC (Rudnick and Gao, 2003), CC (Rodnick and Fountain, 1995), and the source terrains of parent rocks and the tectonic setting of oil shale were determined using various ratios (Hayashi et al., 1970; Ishiga and Dozen, 1977; Bhatia, 1983) and diagrams (Shaw, 1968; Irvine and Bragar, 1971; Gill, 1981; Maynyard et al., 1982; Bhatia, 1983; Le Bas et al., 1986; Roser and Korsch, 1986; Roser and Korsch, 1988; Murphy, 2000; Le Maitre et al., 2002; Campos Neto et al., 2011; Verma and Armstrong-Altrin, 2013). The obtained results were adapted to the geodynamic evolution of the study areas, as well as the petrographic features of volcanism related to the parent rocks that are described in the published literature.

Results

Major elements. The SiO_2 content in the analyzed samples is 45.72–55.55 % (mean = 49.81 %). The value of this major compount gradually decreases from the North Gobustan to the southeast. In addition to SiO_2, the second major compound is Al_2O_3 identified in the composition of samples. The concentration of both compounds reach the maximum level in the mud volcano Demirchi located in the allochthonous.

The Al_2O_3 value varies from 12.69 to 16.81 % (mean = 14.64 %). According to the results of the comparison of all samples, the concentration of Fe_2O_3 in the sample Kichik Siyaki is significantly higher (13.54 %). In the remaining nine analyzed samples, its concentration is characterized by lower values (4.92–8.54 %). The concentration of all other major compounds and their average value are shown in Table 1. In general, the patterns of distribution of major compounds in the samples were determined as follows: $SiO_2 > Al_2O_3 > Fe_2O_3 > CaO > K_2O > SO_3 > MgO > Na_2O > TiO_2 > P_2O_5 > MnO$.

Fig. 4 shows the major element and compound enrichment of samples normalized to PAAS (Taylor and McLennan, 1985), UCC (Rudnick and Gao, 2003) and CC (Rudnick and Fountain, 1995). Compared to PAAS, the samples are significantly enriched in CaO, TiO_2 and MnO, and are relatively enriched in other major oxides (Fig. 4, a). Compared to UCC, slight depletion in SiO_2 and MnO, and enrichment in other major oxides are recorded (Fig. 4, b). The amount of Na_2O is considerably depleted in the samples normalized to UCC and CC (Fig. 4, b and c). Compared to CC the samples show relative enrichment in K_2O, depletion in MgO, slight enrichment in TiO_2, and depletion in SiO_2, P_2O_5 and MnO (Fig. 4, c).

Major and trace element concentrations of oil shale samples

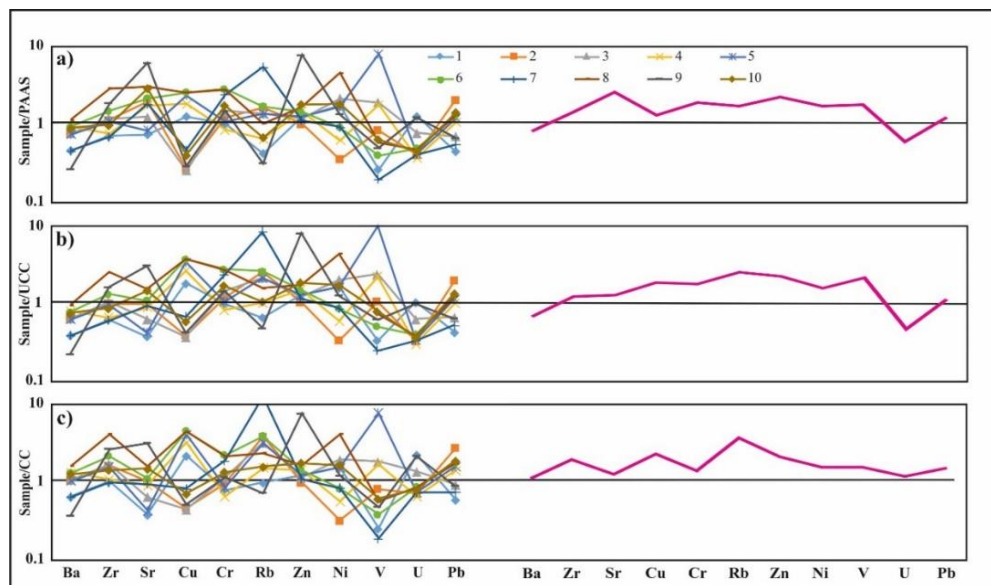| Area	Shamakhi–Gobustan region						Absheron Peninsula			
	Kichik Siyaki	Jəngichay	Shikhzarli	Demirchi	Bozaakhtarma	Qotur	Otmanbozdagh	Lokbatan	Bozdagh–Qobu	Keyreki
Sample	1	2	3	4	5	6	7	8	9	10
Major oxide (wt %)										
SiO$_2$	46.04	49.55	53.39	55.55	51.23	46.43	49.71	46.07	54.39	45.72
Al$_2$O$_3$	13.36	15.36	16.06	16.81	14.93	12.69	15.10	12.96	15.27	13.82
Fe$_2$O$_3$	13.54	4.92	7.29	5.53	8.54	4.97	5.63	5.42	5.46	7.12
FeO	12.18	4.43	6.56	4.98	7.68	4.47	5.07	4.88	4.91	6.41
CaO	1.37	5.22	0.37	2.09	0.29	2.97	7.32	8.47	1.97	9.67
K$_2$O	2.06	3.84	3.65	3.61	3.61	2.93	3.47	3.38	3.89	3.15
SO$_3$	0.45	3.06	3.90	1.26	7.37	4.69	1.69	3.30	3.20	0.35
MgO	2.67	3.20	2.49	2.25	2.58	2.76	2.56	2.81	2.89	2.34
Na$_2$O	1.15	1.38	1.34	1.00	0.97	1.76	1.50	1.63	1.42	1.23
TiO$_2$	0.74	0.75	0.76	0.87	0.71	0.61	0.83	0.66	0.80	0.90
P$_2$O$_5$	0.39	0.04	0.03	0.26	0.03	0.25	0.21	0.25	0.17	0.08
MnO	0.18	0.07	0.09	0.02	0.02	0.05	0.13	0.07	0.07	0.17
Trace elements (ppm)										
Ba	235	405	426	555	384	412	241	516	142	434
Zr	116	196	215	142	184	214	117	419	317	154
Br	8	12	5	1	5	72	5	5	8	3
Mo	80	77	64	48	126	5	19	16	34	12
Sr	116	325	214	317	134	294	295	426	1000	426
Cu	49	11	11	83	94	88	19	89	12	15
Cr	87	112	141	84	96	214	216	212	134	142
Rb	53	218	191	94	175	184	710	114	41	81
Zn	83	71	86	112	85	84	77	100	541	114
Ni	74	16	102	31	75	34	41	176	60	74
Se	0.4	0.1	0.6	0.3	11.6	0.7	0.3	0.5	0.1	0.4
As	5	3	5	8	2	7	23	3	9	7
Ga	17	8	15	11	7	12	14	5	8	12
V	31	104	246	241	964	41	24	61	61	71
U	3	1	2	1	1	1	1	1	3	1
Pb	7	34	12	19	19	18	9	18	11	21
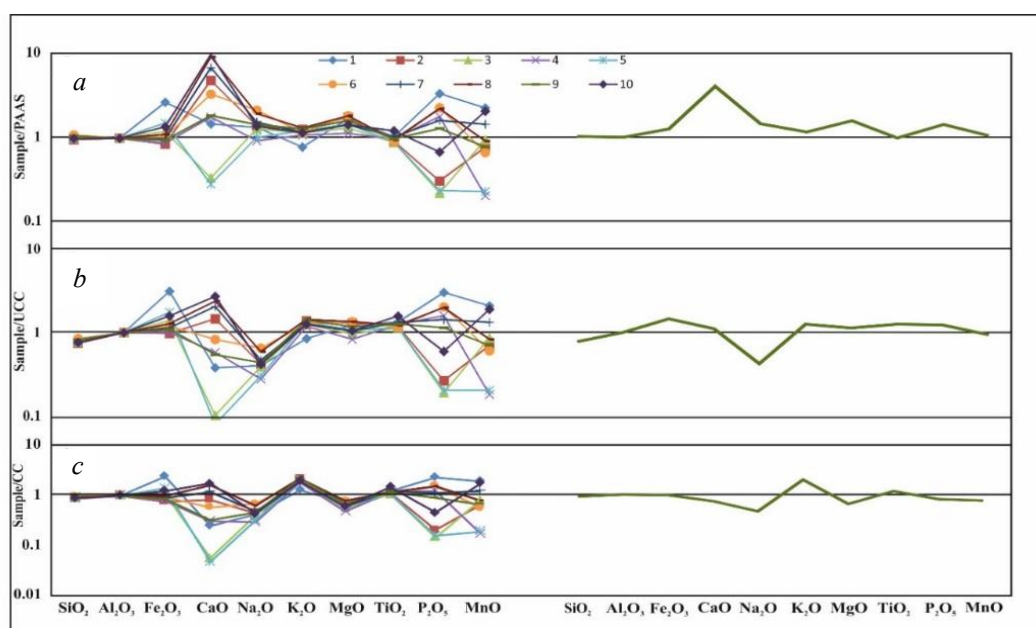
Fig. 4. Major element enrichment of oil shale samples normalized to PAAS (a), UCC (b) and CC (c). The references related to PAAS, UCC and CC are the same in Table 2

Comparison of chemical composition of the studied oil shale with published averages

Chemical content	Present study	PAAS (Taylor and McLennan, 1985)	UCC (Rudnick and Gao, 2003)	CC (Rudnick and Fountain, 1995)
Major oxide (wt %)				
SiO_2	49.81	62.80	66.60	59.10
Al_2O_3	14.67	18.90	15.40	15.80
Fe_2O_3	6.84	7.08	5.04	6.60
CaO	3.97	1.30	3.59	6.40
Na_2O	1.34	1.20	3.27	3.20
K_2O	3.36	3.70	2.80	1.88
MgO	2.65	2.20	2.48	4.40
TiO_2	0.76	1.00	0.64	0.70
P_2O_5	0.17	0.16	0.15	0.20
MnO	0.09	0.11	0.10	0.11
Trace elements (ppm)				
Sr	355	200	320	325
Ba	375	650	628	390
V	184	150	97	131
Ni	68	55	17	51
Cr	144	110	92	119
Zn	135	85	67	73
Cu	47	50	28	24
Zr	207	210	193	123

Fig. 5. Trace element enrichment of oil shale samples
normalized to PAAS (a), UCC (b) and CC (c). The references related to PAAS, UCC,
and CC are the same in Table 2

Trace elements. The Zr value varies from 116 (Kichik Siyaki) to 419 (Lokbatan) ppm in the studied rocks (mean = 207 ppm). According to general considerations, the amount of this element is 200 ± 100 ppm for fine-grained rocks. (Taylor and McLennan, 1985). The lowest concentration of Cr was in the sample from the Demirci volcano (84 ppm), and the highest in the sample of Otmanbozdag (216 ppm) (mean = 144 ppm). In the sample of Otmanbozdag, the amount of Rb is abnormal (710 ppm). In other samples, its quantity is between 53 (Kichik Siyaki) and 218 (Jangicay) ppm (mean = 186 ppm). The minimum Ni concentration is 16 ppm, which was recorded in Jangichay. For other samples, concentrations were determined between 31 and 176 ppm (mean = 68 ppm). The V values are characterized by sharp variable characteristics (31–964 ppm). The mean is 184 ppm (Table 2).

Fig. 5 shows the results of multi–trace element diagrams for samples. Compared to PAAS and UCC, the normalized patterns of samples show considerable depletions in Ba and U. The enrichment trend is recorded in other trace elements (Fig. 5).

Provenance. It is possible to introduce an idea of protolith feature of rocks based on the chemical and mineral content of siliciclastic sedimentary rocks, including oil shale (Kalsbeek and Frei, 2010). Ancient quartz sources of siliciclastic rocks consist of various sedimentary lithotypic materials (metamorphic oil shale, agillites) and detrital components associated with different crystalline rocks.

Based on the relationship between alkali and silica contents, the application of the "TAS" classification (Le Maitre et al., 2002) suggest that the components of rock samples are mixed with alkaline and calc-alkaline series, in more detail, the Jangichay sample refers to trachy-basalat, Shikhzarli, Demirchi and Bozdagh-Qobu to basalt-andesite, and other samples to basalt (see Fig. 6).

The content of Al_2O_3 and TiO_2 provide important indicators for assessing of the provenance features of sedimentary rocks. The remains of Al and Ti in the process of weathering are practically immobile. This is due to the low solubility of their oxides and hydroxides at low temperatures in aqueous solvents (Sugitani et al., 1996). Based on the Al/Ti content in the study rocks, this factor suggests an indication of the type of parent rocks. In the remains of detritus of volcanic rocks, Al is most often associated with feldspars, Ti with ilmenite, olivine, pyroxene, and other mafic minerals. It was determined such regularity by the fact that an increase in the Al/Ti content in rocks is directly proportional to an increase in the SiO_2 content (Holland, 1984). If the Al_2O_3/TiO_2 ratio is between 3 and 8 (the SiO_2 content is 45–52 %), this implies a connection with the mafic, 8–21 (the SiO_2 content 53–66 %) with t he intermediate

compound, 21–70 (the SiO_2 content 66–76 %) with the felsic igneous rocks (Hayashi et al., 1997). The Al_2O_3/TiO_2 ratio is 18.05–21.13 in the samples, and the content of SiO_2 is 45.72–55.55 % (Table 1). The application of this approach suggests that related to the ratio Al_2O_3/TiO_2, all samples correspond to intermediate igneous rocks, but relate to SiO_2 almost identically to mafics.

To clarify the protholit of oil shale, another diagram proposed by Le et al., (1986) was applied in the study. The results show that the samples of Shikzarli, Demirchi, and Bozdagh-Qobu volcanoes correspond to intermediate and others to mafic igneous rocks (Fig. 7).

The most widely used approach to the study of the properties of parent rocks is based on the application of the discriminant function diagram proposed by Roser and Korsch (1988). The application of the diagram shows that the analyzed samples are plotted on the junction line P1-P2 (Fig. 8). The P1 (mafic) characterizes first-cycle basaltic and low-andesitic, and the P2 (intermediate) – rich andesitic detritus features (Roser and Korsch, 1988).

Fig. 9a shows the association with shoshonite in the diagram SiO_2 versus K_2O. High alkalinity is characteristic for shoshonite, and for samples of oil shale the values of the total alkali metals range from 3.21 to 5.31 % (Table 1). In addition, shoshonite contains potassium-rich trachy-andesite, as well as Rb, Sr, Ba, and other trace elements. This fact is confirmed by the determined geochemical composition of samples (Table 1). According to a general tectonic specification, shoshonite igneous rocks show a genetic feature associated with calc- alkaline island-arc subduction volcanism. K-rich shoshonite rocks are younger and occur above deeper or steeper parts of the Benioff subduction seismic zone. (Müller and Groves, 2019).
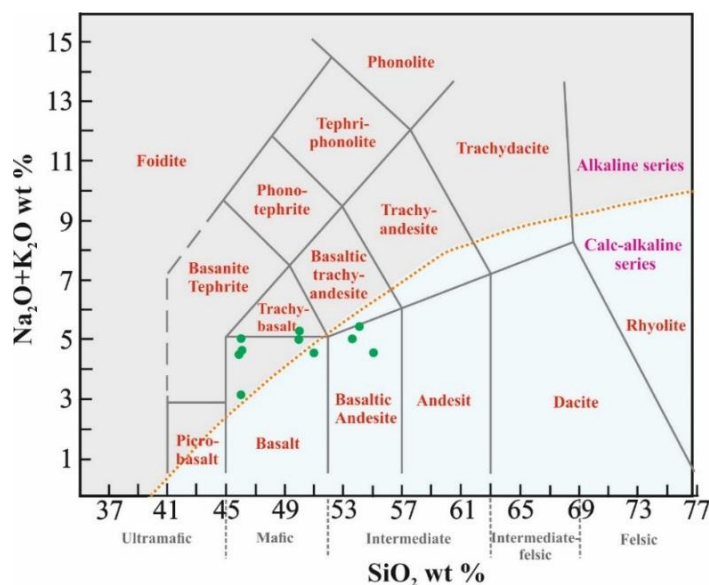

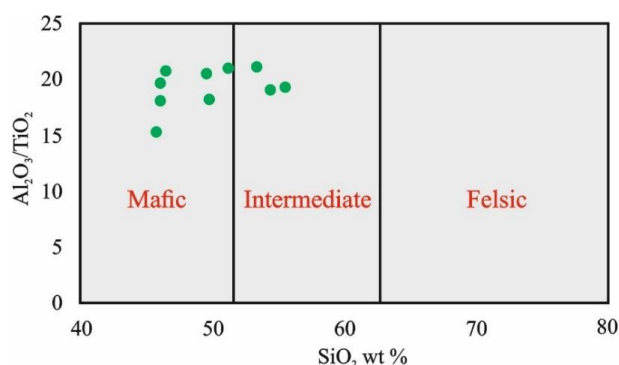**Fig. 6.** Total alkali versus silica (TAS) diagram of samples

Fig. 7. Association of samples with mafic and intermediate magmatic rocks: the result of SiO_2 versus Al_2O_3/TiO_2 diagram (Le Bas et al., 1986)
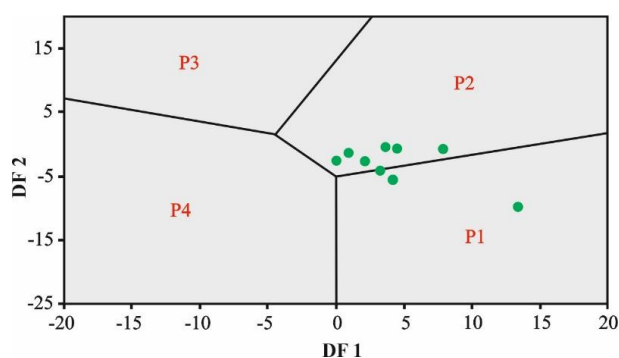

Fig. 8. Classification plot (Roser and Korsch, 1988) of discriminant function 1 (DF 1) and discriminant function 2 (DF 2) for the samples:
$DF\ 1 = (–1.773 × TiO_2\ \%) + (0.607 × Al_2O3\ \%) + (0.76 × Fe_2O_3\ T\ \%) + (–1.5 × MgO\ \%) + (0.616 × CaO\ \%) + (0.509 × Na_2O\ \%) + (–1.22 × K_2O\ \%) + (–9.09); DF\ 2 = (0.445 × TiO_2\ \%) + (0.07 × Al_2O_3\ \%) + (–0.25 × Fe_2O_3\ T\ \%) + (–1.142 × MgO\ \%) + (0.432 × Na_2O\ \%) + (1.426 × K_2O\ \%) + (–6.861).$
P1 – Mafic magmatic origin; P2 – Intermediate magmatic origin; P3 – Felsic magmatic origin; P4 – Continental sedimentary origin
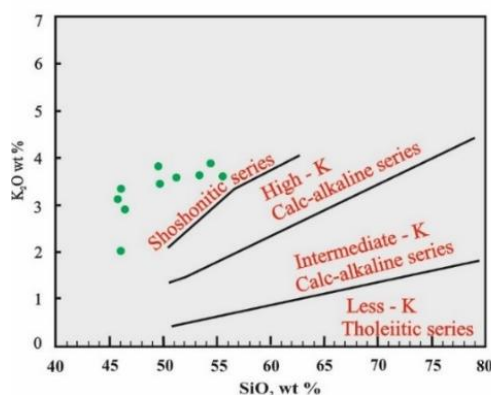
a
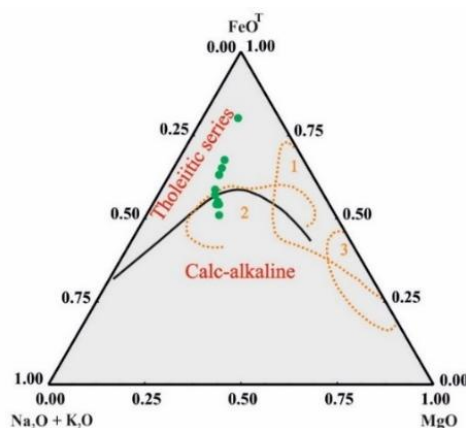
b

Fig. 9. SiO_2 versus K_2O diagram (Gill, 1981) (a) and $(Na_2O + K_2O) – FeO$ (total) – MgO ternary diagram (Irvine and Bragar) (b) for the samples: fields for (1) island arc non–cumulates, and (2) island arc cumulates after Beard (1986) and (3) ophiolites/cumulates after Coleman (1977) are shown for comparison

The result of the diagram of total alkalis $(Na_2O + K_2O) – FeO^*$ (total Fe as FeO) – MgO suggest the samples of Lokbatan, Bozdagh-Qobu, Qotur and Jangichay correspond to calc-alkaline, and other samples to tholeiitic basalts (Fig. 9, *b*). Calc-alkaline rocks are mainly found in arcs above the subduction zones, usually in volcanic arcs on continental crust. Tholeiitic series rocks are characteristic of igneous rocks erupted by submarine volcanism in mid-ocean ridges, and make up most of the oceanic crust.

High concentrations of Ni play a major role in the formation of chloride, which is a product of the pyroxene mineral. Together with V and Cr, these three elements have the same features during fractional eruption processes and are used as an indicator to evaluate the provenance features of sedimentary rocks associated with mafic or ultramafic volcanogenic composition. In contrast to the parent rocks associated with felsic origin, their concentrations are high in mafic and ultramafic content.

Compared to PAAS, UCC, and CC, the samples show enrichment in all three trace elements (Table 2, Fig. 5). For the ultramafic composition of the parent rock, a high Cr content is an indicator of the presence of components rich in pyroxene, while Ni is rich in olivine (Huntsman-Mapila et al., 2005). The richness of Cr in shale is associated with chrome spinels. In addition to Ni, the Cr content indicates the contact of Cr and Ni ions with clay particles during weathering of ultramafic rocks containing chromites (Garver et al., 1996). The positive relationship (r = 0.28) obtained as a result of the correlation between these two trace elements for shale samples, is indication of the association with mafic or intermediate source terrains.

Like Na, the Ti content is considered an indicator of basic or intermediate composition. The abundance of Zr reflects the origin of the source associated with felsic (Ishiga and Dozen, 1997). The vertical curves were constructed on the basis of Ti/Zr and Cr/Zr ratios, in order to clarify the sources of parent rocks for oil shale samples. Analysis of these curves suggest that the samples of Lokbatan and Bozdagh-Qobu are associated with felsic, Otmanbozdagh with mafic, and others with intermediate igneous composition (Fig. 10).

K and Rb are known for their mobile properties under metamorphic conditions characterized by diagenesis and low temperatures (Shaw, 1968). In this regard, the results of Fig. 11 show that, unlike the sample of Kichik Siyaki, other samples were derived from acidic and intermediate sources.
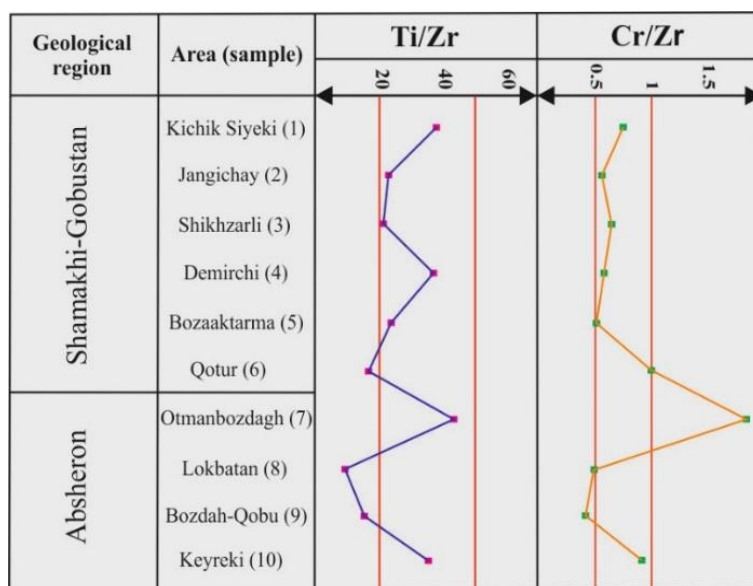

Fig. 10. Vertical curves based on Ti/Zr and Cr/Zr ratios
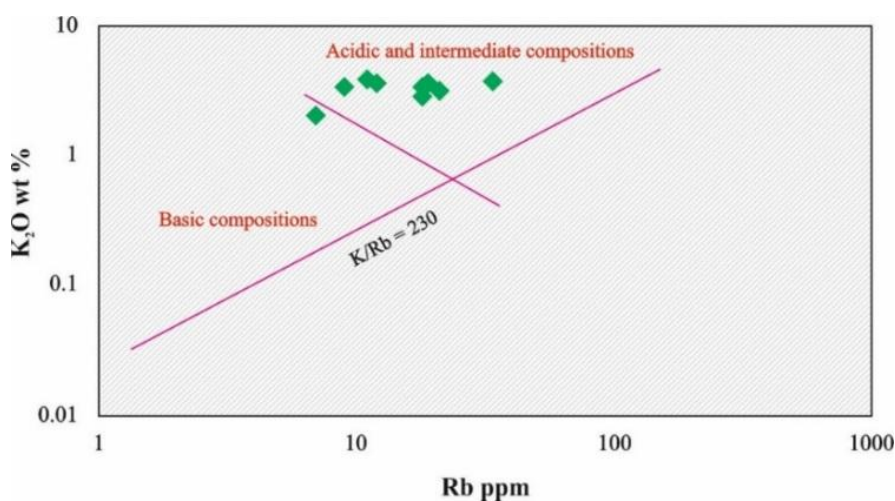for samples: Ti/Zr > 50 – mafic; < 20 – felsic; Cr/Zr > 1 – mafic; < 0.5 – felsic

Fig. 11. Bivariate plot of K_2O versus Rb of oil shale samples
relative to a K/Rb ratio of 230 (main trend of Shaw, 1968)

Tectonic setting. Bulk rock geochemistry of sediments also provides useful information for their palaeotectonic setting. The content of SiO_2 and their K_2O/Na_2O ratio are used to establish the tectonic classification of shale and other sedimentary rocks. In accordance with several possible sedimentation settings, three first-order tectonic categories (passive continental margin, active continental margin, and oceanic island arc) have been identified. Quartz-rich and mineralogical mature sedimentary rocks fall into the first category, in which sediments are derived from stable continental margins or intracratonic basins (Roser and Korsch, 1986). According to Bhatia (1983), the main characteristics that distinguish the chemical composition of passive continental margin are: enrichment in SiO_2, depletion in Al_2O_3, TiO_2, Na_2O, and CaO, as well as Ka_2O/Na_2O ratio > 1. Since the samples are characterized by an intermediate content of quartz (Table 1), they should be associated with a deposition that occurred at the active continental margin or active plate boundaries (Roser and Korsch, 1986). The rocks in the Andean types of active continental margins are similar to in the basement uplift. Their composition is identical to the UCC. In such geotectonic areas, the values of SiO_2 and K_2O prevail, and the ratio of K_2O/Na_2O is approximately equal to 1 (Bhatia, 1983).

Quartz-poor sedimentary rocks are related to oceanic island arc (Roser and Korsch, 1986). They are characterized by calc-alkaline andesitic composition. High concentrations of TiO_2, Al_2O_3, Na_2O, and Fe_2O_3 are established in this type of tectonic environment. Hence the amount of SiO_2 and K_2O is less than that of others (Bhatia, 1983).

Considering the noted specific and distinctive features, including the silicate composition and immobile or relatively mobile major oxides of rocks, a number of tectonic diagrams are proposed for studying the palaeoectonic properties. Thus, the diagram proposed by Maynard et al. (1982) is based on a graphical relationship between the content of alkali metal oxides, such as K and Na, and the ratio of SiO_2/Al_2O_3 in rocks. The ratio of SiO_2/Al_2O_3 is an indicator of the richness of quartz, and the ratio of K_2O/Na_2O reflects the amount of mica and K–feldspar compared to the content of plagioclase in rocks. If we estimate the paleotectonic properties of the samples using this approach, the result assumes a connection with the active continental margin (Fig. 12, *a*). In addition, since Si/Al < 5 and K/Na < 1 are characteristic of an active continental margin, and Si/Al < 5 and K/Na > 1 of an continental collision, then the paleotectonic setting of samples can be associated with an active continental margin, as well as a continental collision (Fig. 12, *b*).

The most widely used discriminant diagram in the published literature, based on the mobile or relative immobile chemical composition of rocks, proposed by Roser and Korsh (1986), is related to the interaction between the SiO_2 value and the K_2O/Na_2O ratio. Using the same parameters, Murphy (2000) proposed another diagram. The analysis carried out in both diagrams suggests that the tectonic nature of the samples is associated with active continental margins (Fig. 13, *a* and 13, *b*), which means an unstable continental state.

All the selected samples are plotted in the field of the active continental margin based on the discriminant function diagram proposed by Bhatia (1983), which is related to the use of multi-geochemical parameters compared to other approaches (Fig. 14). DF 1 and DF 2 are determined by the formula [DF 1 = $-0.0447 \times SiO_2 - 0.972 \times TiO_2 + 0.008 \times Al_2O_3 - 0.267 \times Fe_2O_3$ (total) $+ 0.208$ FeO (total) $- 3.082 \times MnO + 0.140 \times MgO + 0.195 \times CaO + 0.719 \times Na_2O - 0.032 \times K_2O + 0.303$. DF 2 = $= -0.421 \times SiO_2 + 1.988 \times TiO_2 - 0.526 \times Al_2O_3 - 0.551 \times Fe_2O_3 - 1.61 \times FeO$ (total) $+ 2.720 + MnO + 0.881 \times MgO - 0.907 \times CaO - 0.177 \times Na_2O - 1.840 \times K_2O - 7.244 \times P_2O_5 + 43.57$]. The process of sedimentation occurs in arcs associated with subduction characteristic of such active continental slopes. In addition, the marginal strike-slip dislocations, and sedimentation processes taking place near back-arc basin are very typical for such paleotectonic condition (Alvarez and Roser, 2007).
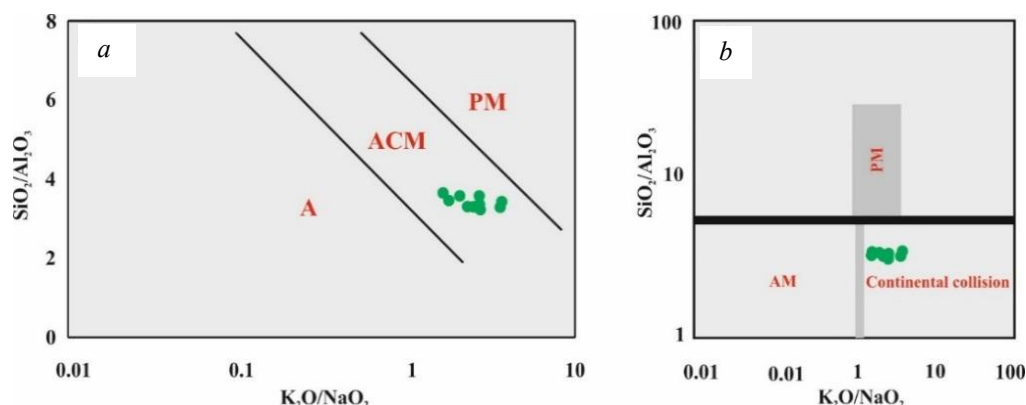

Fig. 12. Tectonic discriminant diagrams based on K_2O/Na_2O and SiO_2/Al_2O_3 ratios for oil shale samples: a – PM – continental margin, ACM – active continental margin, A – arc (Maynyard et al., 1982); b – PM – continental margin, AM – active continental margin (Campos Neto et al. 2011)
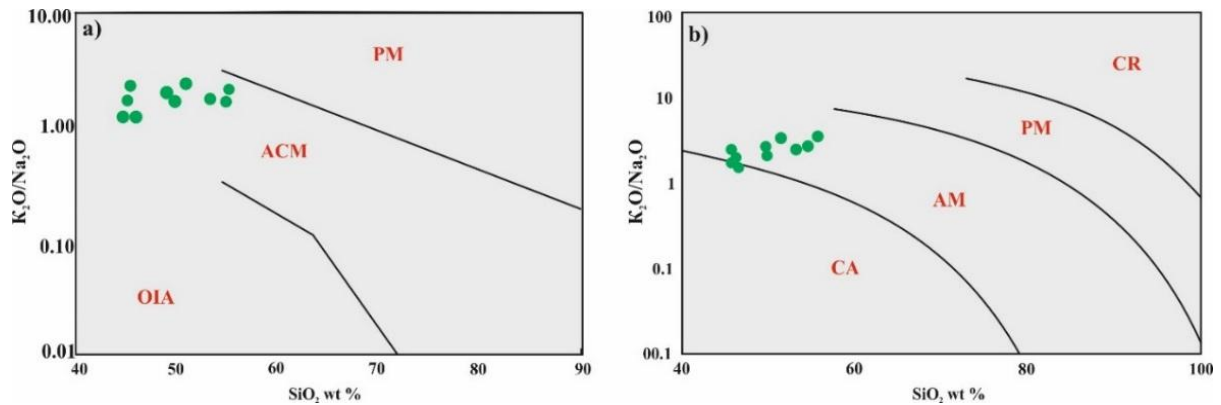
Fig. 13. Tectonic discriminant diagrams are based on the interaction between the SiO_2 value and the K_2O/Na_2O ratio for oil shale: a) PM – passive margin, ACM – active continental margin, OIA – oceanic island arc (Roser and Korsch, 1986); b) CR – continental rift, PM – passive margin, AM – active margin, CA – continental arc (Murphy, 2000)
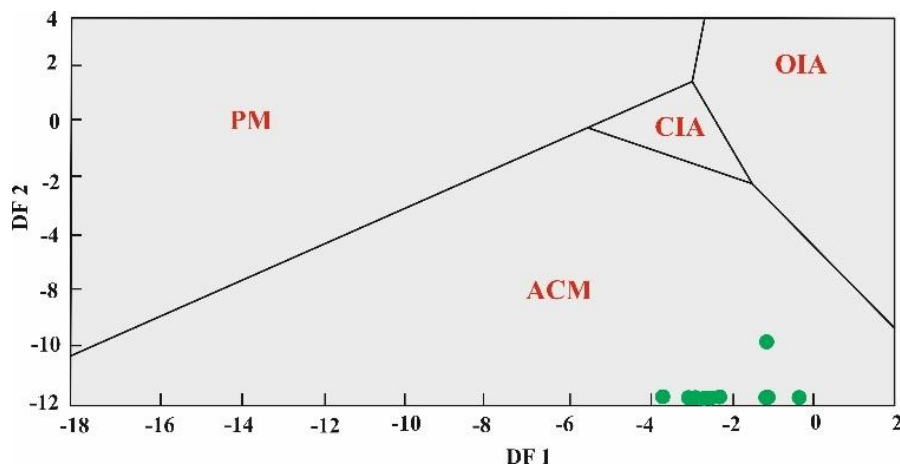

Fig. 14. Tectonic discriminant function multi–dimensional diagram for oil shale samples: PM – passive margin; ACM – active continental margin; CIA – continental island arc, OIA – oceanic island arc (Bhatia, 1983)
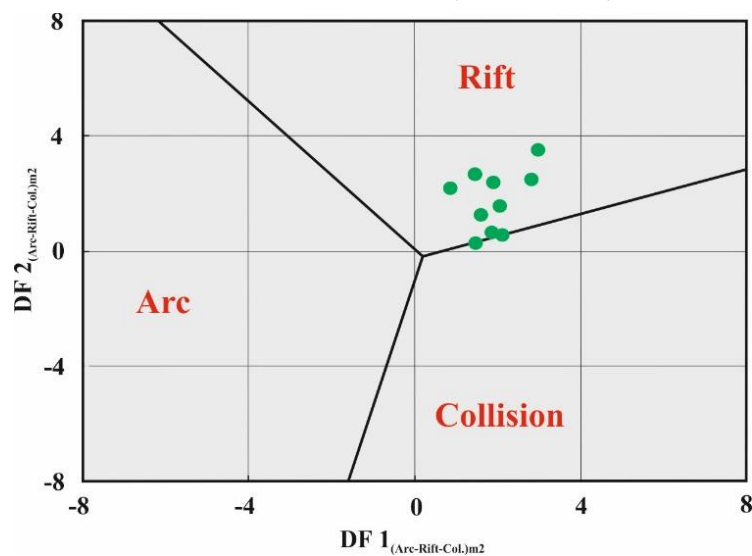

Fig. 15. New discriminant–function multidimensional diagram (Verma and Armstrong–Altrin, 2013) for low–silica samples

Verma and Armstrong-Altrin (2013) established two new discriminant-function-based major element diagrams for the tectonic discrimination of siliciclastic rocks from three tectonic settings: arc, continental rift, and collision, created for the tectonic discrimination of high-silica $[(SiO_2)adj = 63–95\%]$ and low-silica $[(SiO_2)adj = 35–63\%]$ rocks. DF 1 and DF 2 are determined by the formula

$$[DF\ 1_{(Arc–Rift–Col.)m2} = 0.608 \times In(TiO_2/SiO_2)_{adj} +$$
$$+ (-1.854 \times In\ (Al_2O_3/SiO_2)_{adj}) + (0.299 \times$$
$$\times In(Fe_2O_3\ T/SiO_2)_{adj}) + (-0.550 \times$$
$$\times In(MnO/SiO_2)_{adj}) + (0.120 \times In(MgO/SiO_2)_{adj}) +$$
$$+ (0.194 \times In(CaO/SiO_2)_{adj}) + (-1.510 \times$$
$$\times In(Na_2O/SiO_2)_{adj}) + 1.941 \times In(K_2O/SiO_2)_{adj} +$$
$$+ (0.003 \times In(P_2O_5/SiO_2)_{adj}) - 0.294.$$

$$DF\ 2_{(Arc–Rift–Col)m2} = (-0.554 \times In(TiO_2/SiO_2)_{adj} +$$
$$+ (-0.995 \times In\ (Al_2O_3/SiO_2)_{adj}) +$$
$$+ (1.765 \times In(Fe_2O_3\ T/SiO_2)_{adj}) + (-1.391 \times$$
$$\times In(MnO/SiO_2)_{adj}) + (-1.034 \times$$
$$\times In(MgO/SiO_2)_{adj}) + (0.225 \times In(CaO/SiO_2)_{adj}) +$$
$$+ (0.713 \times In(Na_2O/SiO_2)_{adj}) + (0.330 \times$$
$$\times In(K_2O/SiO_2)_{adj}) + (0.637 \times In(P_2O_5/SiO_2)_{adj}) -$$
$$-3.631].$$

Due to the high silica content, which does not coincide with the composition of oil shale samples (table 1), the second condition was taken into account when creating the diagram. The samples plot near a line that separates the rift and collision fileds. The result of the diagram shows a transition tendency, which is interpreted as a rift-to-collision transition (Fig. 15).

Results and discussion

The results obtained from the normalized multi-element spider diagrams (Fig. 4 and Fig. 5) and the other plots (Fig. 12, *a*, 13, *a*, *b* and Fig. 14) based on major oxides suggest the active continental margin setting, which provides good evidence for the slopes of continental crust of the South Caucasus Plate (Pontides-South Caucasus-Transcaspian microcontinent).

The application of the plot related to the K_2O/Na_2O ratio versus the SiO_2 value (Fig. 12, *b*), and the discriminant-function multidimensional diagram (Fig. 15) support the geodynamic environment, which corresponds to the collision on the continental margin or the transition from rifting to collision.

The study of published literature indicates that at each transitional geodynamic stage of the J_1-P_2, the central independent graben zone (shale-flysch-rift-related basin including its Goytkh-Tufan axial zone), which was a suboceanic crust of the southern slope of the Greater Caucasus, as well as known as a zone of divergence between the South Caucasus-Transcaspian and the Scythian-Turan plates, migrated to the south and completely closed in the upper Eocene (Brunet et al., 2003; Khain, 1950; Aliyev et al., 2005; Rustamov, 2008). The process led to the formation of a tectonic

criterion for the beginning of continental collision conditions (Rustamov, 2015), which is confirmed in Fig. 12, *b*.

Thus, the basin-forming conditions for the samples of the Middle Eocene may be related to the final Paleocene-Eocene basin, which was the northern branch of Meso-Tethys in the Crimea-Greater Caucasus-Kopetdag system. More specifically, evolution of that independent deepwater basin, fed on the left-north branch of Meso-Tethys (Rustemov, 2005; Rustemov, 2008) is associated with areas covering the shale-flysch trough of the axial zone, which formed as a result of rifting occurred in Jurrasic (Zonenshain and Le Pichon, 1986; Khain, 1994; Babayev et al., 2015) in the North Crimea-Greater Caucasus-Kopeh Dagh system, and extended to the east of Kopeh Dagh. The shale-flysch and non-compensated (Babayev et al., 2015; Rustemov, 2015) deep basin played the role as a border between the Scythian-Turan plate of Eurasian continent and the intra-Transcaucasian plate. In addition, in the published literature (Rustemov, 2005; Rustemov, 2008; Rustemov, 2015), three phases were established, which related to the evolution of collision in the study area. The considered scenario of sedimentation for the Middle Eocene corresponds to the initial soft phase of the collision (Rustemov, 2015), which is confirmed in Fig. 15.

The diagrams and ratios used for major and trace elements in the composition of oil shale support the feature of mafic-intermediate protolith. Thus, according to the "TAS" diagram, the samples show alkaline and calc-alkaline characteristics (Fig. 6). The diagram of SiO_2 versus K_2O shows correspondence with the K-rich shoshonite (Fig. 9, a) and the $Na_2O + K_2O - FeO$ (total) diagram indicates the source of the calc-alkaline and tholeiitic series (Fig. 9, *b*). In general, the samples of oil shale are characterized by mixed properties of basalt and basaltic andesite.

The diagrams based on the trace element content of oil shale also confirm the mafic-intermediate protolith (Fig. 10 and 11). If we investigate the provenance characteristics of the samples belonging to the study areas, as well as the Paleocene-Eocene basin, then the role of basaltic-andesitic volcanism in the Cimmerian and Alpine tectogenesis on the southern slopes of the Greater Caucasus (in the Tufan and Vandam uplifts) should be taken into account.

In connection with subduction (the sub-oceanic crust of the Greater Caucasus, including the Tufan Basin zone moved under the Scythian Plate) continued up to the Toarcian age, the evolution of the shale-flysch trough (with a thickness of 10 km (Babayev et al., 2015)) in the Lias-Aalenian age, and finished with closure and transformation into a submarine accretionary prism in the Bajocian stage. All these processes led to a gradual migration of the trough (to the south) in the period from the Upper Jurassic to the Lower Cretaceous. In the central part of the trough, due to fissure magmatism in the Early

Jurassic and Alenian periods, 500 meters of tholeiitic-basalt products were accumulated (Babayev et al., 2015), which justifies the result obtained in Fig. 9, *b*. The published literature also reports (Aliyev et al., 2005; Rustamov, 2005; Rustamov, 2008; Babayev et al., 2015) the formation of an accretionary prism complex and the basalt-andesite series of rift volcanism on the active margins of the Scythian plate. The Tufan uplift located in the south of the Main Caucasian thrust, as well as in the accretionary prism zone, as a fragment of the axial zone of the deepened and expanded trough, has played the role of space for the widespread expansion of calc-alkaline (andesite-dacite-rhyolite) volcanism in the Bajocian stage (Babayev et al., 2015). For this type of igneous rock, an average depth (up to 30 km) and upper intervals of subduction zones are characteristic (Kondiy, 1997). Considering the geodynamic process that occurred in the Jurassic period in the uplift of Tufan, and the original source of detrital materials, it can be concluded that the major regularities defined for the Greater Caucasus-Kopeh Dagh system are: the tectonic folding phases, which occurred before the Bajocian stage; the formation of large-scale accretion prism sediments; and island arc volcanism took place in the basin of axial zone (to the Scythian-Turan plates). One of the reasons for the migration of the deeper central graben zones to the south is subduction, tilted to the south, and another is the tension between the South Caucasus and the Scythian (southern margin of the Eurasian continent) plates. The magmatism, occurred at the active margin of the Scythian Plate, and the southern island part of the Greater Caucasus basin decreased to the east. Therefore their absence in the Kopeh Dagh was associated with a decrease in the subduction velocity in this direction (Rustamov, 2005).

Related to processes: the transgressive extension of Meso-Tethys in the Barremian age; the gradual movement of flysch deposits to the south on the southern slope of the Greater Caucasus and Absheron Sill; as well as the narrow flysch localization (strip-shaped) on the southern margin of the Dubrar Trough (Khain, 1950) led to the formation of a depression characterized by the subduction, tilted to the south. In the Early Albian age, the sedimentation process continued into the depression. The axial zone of the Dubrar Trough moved under the Kakheti-Vandam zone, which is located on the north margin of the South Caucasus Plate. As a result of subduction, at the beginning of the continental rifting process in the Kakheti-Vandam zone, after the late Albian period, Andean type volcanism occurred, consisting of subalkaline basalt (olivine) series. This type of volcanism continued for short-term intervals, during the Cenoman-Turonian periods of the Late Cretaceous. The second type of volcanism consisted of shoshonite-latite series was defined (Abdullayev et al., 1991) at the early Senonian age. Deep depths (over 25 km)

and surface zone of deeper subduction are typical of these eruptive products (Kondiy, 1997). Unlike the Vandam zone, volcanic processes are weakened as a result of the weakening of endogenous processes in the direction of Kakheti. However, the fragmentation processes associated with dislocation in this zone are poorly preserved, which led to the formation of an edge magmatic chamber (magmatic sources) consisting of subalkaline composition (Rustamov, 2008). Thus, the second (the last) parent rock source of oil shale corresponds to the rift-related basaltic volcanism of the Albian-Cenomanian and the Senonian ages of the Cretaceous. Their existence in the Vandam zone is associated with marginal continental type of geodynamic evolution, and the activation of meridional tectonic faults of the intraplate, occurred on the slopes of the Transcaucasus microcontinent on the southern flank of the flysch basin (Kakheti-Vandam zone). Some published literature (Aliyev et al., 2005; Babayev et al., 2015) also provides information on the prevalence of volcanic-detrital, lava, and subvolcanic facies of Alb-Cenomanian and Senonian ages in the Vandam zone.

The beginning of the late Alpine tectogenesis corresponds to the period of regional uplift in the Caucasus-Caspian region and Iran (Shixalibeyli, 1967; Rustamov, 2008; Babayev et al., 2015). The flysch basin of Meso-Tethys covered the southern slopes of the Greater Caucasus and the Absheron Sill, played a role in transporting volcanogenic detrital materials from the Tufan and Vandam uplifts was completely closed in the Upper Eocene. (Brunet et al., 2003; Rustamov, 2015). In the tectonic phase of Laramie (Babayev et al., 2015), the complete closure of other ocean basins in the Mediterranean zone, including the Zagros-Caucasus segment, led to the transformation of Meso-Tethys into Neo-Tethys (Rustamov, 2015). After a relative weakening of geodynamic and magmatic processes, the collision of continents occurred in the phase of Laramie (the Late Cretaceous-Paleogene transitional stage) of Alpine tectogenesis, which led to the predominance of the initial collision conditions (Belov et al., 1990; Milanovsky, 1991; Ershov et al., 2003; Rustemov, 2005; Rustemov, 2008). The evolution of the collision occurred in the widespread shallow-seabed conditions of Neo-Tethys, including intraplate tectonic setting (Rustamov, 2015).

Conclusion

The oil shale samples demonstrate the basalte and basaltic andesite protolithic nature, which supports the conclusion that original volcanogenic detrital materials were derived from mafic and intermediate source terrain.

The bulk rock geochemistry data of samples show an active continental margin setting, which suggests

55

the idea that the spatial formation of samples associated with continental crust, the slopes of the South Caucasus Plate. The results obtained from the diagrams based on palaotectonic settings suggest the rift-to-collision transition or palaeogeodynamic conditions of the initial collision.

The evolution of oil shale is associated with the formation of a shale-flysch trough in the axial zone, which related to the rift process occurred in North Crimea-Greater Caucasus-Kopeh Dagh system (in the Lias-Aalenian age), including an independent deep-water basin, which fed on the left-north branch of Meso-Tethys and extending to the east of Kopeh Dagh. At each transitional geodynamic stage of the J_1-P_2, the suboceanic basin of the the southern slope of the Greater Caucasus limited by listric faults of the active margin of the Eurasian continent and South Caucasus Plate, gradually migrated to the south and completely closed in the Upper Eocene. The process led to the formation of a geotectonic criterion for the beginning of the continental collision conditions. This considered scenario of sedimentation in the Middle Eocene corresponds to the initial soft phase of the collision.

In connection with the provenance nature of basalt and basaltic andesite source terrain and the possible prospect of the Middle Eocene basin, the role of the basaltic-andesitic subduction volcanism in the Cimmerian and Alpine tectogenesis on the southern slopes of the Greater Caucasus (the Tufan and Vandam uplifts) is considered decisive. Thus, the Tufan uplift, located in the accretionary prism zone played the role of a primary space for the wide distribution of calc-alkaline island volcanism in the Bajocian stage of the Jurrasic. The final volcanogenic detrital source of oil shale associated with to the rift-related subalkaline basaltic (olivine) and shoshonite-latite series volcanism of the Albian-Cenomanian and the Senonian ages of the Cretaceous in the Vandam zone. The volcanism was associated with the marginal continental type of geodynamic evolution and the activation of meridional tectonic faults in intraplate environments.

References

Abbasov, O. R. (2009). Distribution regularities of shales of Paleogene–Miocene sediments in Gobustan (Abstract of PhD thesis … on PhD in Earth Sciences). 26.11.09 / O. R. Abbasov [Institute of Geology and Geophysics, Azerbaijan National Academy of Sciences], Baku.

Abbasov, O. R. (2015). Oil shale of Azerbaijan: geology, geochemistry and probable reserves. *International Journal of Research Studies in Science, Engineering and Technology,* 2(9), 31–37.

Abbasov, O. R. (2016). Geological and geochemical properties of oil shale in Azerbaijan and petroleum potential of deep-seated Eocene-Miocene deposits. *European journal of natural history*, 2, 31–40.

Abbasov, O. R. (2016). Distribution regularities of oil shale in Azerbaijan. *ISJ Theoretical & Applied Science, 3*(35), 165–171. doi: http://dx.doi.org/10.15863/TAS.2016.03.35.28

Abbasov, O. R. (2017). Distribution regularities and geochemistry of oil shales in Azerbaijan. *Mineral resources of Ukraine, 2*, 22–30.

Abbasov, O. R., Baloglanov, E. E. & Akhundov, R. V. (2015). *Organic compounds in ejected rocks of mud volcanoes as geological and geochemical indicators: a study from Shamakhi-Gobustan region (Azerbaijan).* Azerbaijan, Baku: International Multidissiplinar Forum "Academic Science Week-2015".

Abbasov, O. R., Mamedova, A. N., Huseynov, A. R. & Baloglanov, E. E. (2013). Some new data of geochemical researches of combustible slates of Azerbaijan. *Geology, geophysics and development of oil and gas fields, 2*, 32–35.

Abdullayev, R. N., Mustafayev, M. A., Samedova, R. A., Shafiyev, Kh. I. & Memedov, M. N. (1991). Petrology of the magmatic complexes of the southern slope of the Greater Caucasus (Vandam zone). Baku: Publishing house "Elm".

Aliyev, Ad. A., Abbasov, O. R., Ibadzade, A. J. & Mammadova, A. N. (2015). Prospects of using of Azerbaijan oil shale. *Proceedings of the Azerbaijan National Academy of Sciences*, 2 (1), 43–47.

Aliyev, Ad. A. & Abbasov, O. R. (2016). Alternative fuel and energy resources of Azerbaijan. *International Azerbaijan Journal*, 2 (80), 56–62.

Aliyev, Ad. A., Abbasov, O. R., Ibadzade, A. J. & Mammadova, A. N. (2018). Genesis and organic geochemical characteristics of oil shale in eastern Azerbaijan. *SOCAR Proceedings, 3*, 4–15. doi: 10.5510/OGP20180300356

Aliyev, Ad. A., Abbasov, O. R., Ibadzade, A. J. & Mammadova, A. N. (2018). Organic–geochemical study of oil shales in Pre–Caspian–Guba region (Azerbaijan). *Mineral resources of Ukraine, 3,* 13–18. https://doi.org/10.31996/mru.2018.3.13–18

Aliyev, Adil & Abbasov, Orhan (2018). *Organic geochemical characteristics of oil shale in Azerbaijan.* Tehran, Iran: The 36th National and the 3rd International Geosciences Congress.

Aliyev, H. A., Ahmedbeyli, F. S., Ismayilzade, A. J., Kengerli, T. N. & Rustamov, M. I. (2005). *Geology of Azerbaijan,* (Vol. IV, 506 p.). Baku: "Nafta-Press" Publishing house.

Aliyev, Ad. A., Aliyev, Ch. S., Feyzullayev, A. A., Huseynov D. A., Isayeva M. I., Gadirov F. A. & Novruzov, N. A. (2015). *Geology of Azerbaijan* ,(Vol. II, 341 p.). Baku: Publishing house "Elm".

Aliyev, Ad. A., Bayramov, A. A., Abbasov, O. R. & Mammadova, A. N. (2014). Reserves of oil shale

and natural bitumen. National Atlas of the Republic of Azerbaijan, Map (Scale 1:1000000), 101.

Aliyev, Ad. A. & Bayramov, A. A. (1999). Some aspects of the tectonics of the Gobustan mud volcanic zones. *Proceedings of ANAS, Earth Sciences, 1, 129-131.*

Aliyev, Ad. A., Guliyev, I. S., Dadashev, F. G. & Rahmanov, R. R. (2015). Atlas of mud volcanoes in the world. Baku: Publishing house "Nafta–Press", "Sandro Teti Editore", 361 p.

Alvarez, N. C. & Roser, B. P. (2007). Geochemistry of black shales from the Lower Cretaceous Paja Formation, Eastern Cordillera, Colombia: Source weathering, provenance, and tectonic setting. Journal of South American Earth Sciences, 23(4), 271–289. https://doi.org/10.1016/j.jsames.2007.02.003

Babayev, Sh. A., Bagmanov, M. A., Aliyeva, E. H.–M., Alizade, Kh. A., Kengerli, T. N., Latifova, Y. N. & Zohrabova, V. R. (2015). *Geology of Azerbaijan* (Vol. II, 532 p.). Baku: Publishing house "Elm".

Beard, J. S. (1986). Characteristic mineralogy of arc–related cumulate gabbros: Implications for the tectonic setting of gabbroic plutons and for andesite genesis. *Geology, 14*(10), 848–851. https://doi.org/10.1130/0091–7613(1986)14<848:CMOACG>2.0.CO;2

Belov, A. A., Burtman, V. S., Zinkevich, V. P., Knipper, A. L., Lobkovsky, L. I., Lukianov, A. V. … & Rachkov, V. S. (1990). *Tectonic layering of Lithosphere and Regional Geological Investigations*. Nauka, Moscow.

Bhatia, M. R. (1983). Plate tectonics and geochemical composition of sandstones. *Journal of Geology, 91*(6), 611–627. DOI: 10.1086/628815

Campos Neto, M. D. C., Basei, M. A. S., Assis Janasi, V. D. & Moraes, R. (2011). Orogen migration and tectonic setting of the Andrelândia Nappe system: an Ediacaran western Gondwana collage, south of São Francisco craton. *Journal of South American Earth Sciences*, *32*, 393–406. DOI: 10.1016/j.jsames.2011.02.006

Coleman, R. G. (1977). Emplacement and metamorphism of ophiolites. *Rend. Soc. Ital. Mineral. Petrol., 33* (1): 161–190.

Ershov, A. V., Brunet, M. –F., Nikishin, A. M., Bolotov, S. N., Nazarevich, B. P. & Korotaev, M. V. (2003). Northern Caucasus basin: Thermal history and synthesis of subsidence models. *Sedimentary Geology, 156*, 95–118, doi: 10.1016/S0037–0738(02)00284–1

Garver, J. I., Royce, P. R. & Smick, T. A. (1996). Chromium and nickel in shale of the Taconic foreland: a case study for the provenance of fine–gained sediments with an ultramafic source. *Journal of Sedimentary Research, 66*, 100-106. https://doi.org/10.1306/D42682C5–2B26–11D7–8648000102C1865D

Gill, James. (1981). *Orogenic Andesites and Plate Tectonics*. Springer. 10.1007/978–3–642–68012–0

Hayashi, K. I., Fujisawa, H., Holland, H. D. & Ohmoto, H. (1997). Geochemistry of ~1.9 Ga Sedimentary Rocks from Northeastern Labrador, Canada. *Geochimica et Cosmochimica Acta, 61*(19), 4115–4137. doi:10.1016/s0016–7037(97)00214–7

Hiroaki, Ishiga & Kaori, Dozen. (1997). Geochemical indications of provenance change as recorded in Miocene shales: opening of the Japan Sea, San'in region, southwest Japan. *Marine Geology, 144*(1–3), 211–228. https://doi.org/10.1016/S0025–3227(97)00104–7

Holland H. D. (1984). *The chemical evolution of atmosphere and oceans*. Princeton Univ. Press, Princeton N.J.

Irvine, T. N. & Baragar, W. R. A. (1971). Aguide to the chemical classification of the common volcanic rocks. *Canadian Journal of Earth Sciences, 8*(5), 523–548. https://doi.org/10.1139/e71–055

J. Barry Maynard, Renzo Valloni & Ho–Shing Yu. (1982). *Composition of modern deep–sea sands from arc–related basins*. Geological Society, London, Special Publications, 10, 551–561. https://doi.org/10.1144/GSL.SP.1982.010.01.36

J. Brendan Murphy. (2000). Tectonic influence on sedimentation along the southern flank of the late Paleozoic Magdalen basin in the Canadian Appalachians: Geochemical and isotopic constraints on the Horton *Group in the St. Marys basin, Nova Scotia GSA Bulletin, 112*(7), 997–1011. https://doi.org/10.1130/0016–7606(2000)112<997:TIOSAT>2.0.CO;2

Kalsbeek, F. & Frei, Robert. (2010). Geochemistry of Precambrian sedimentary rocks used to solve stratigraphical problems: An example from the Neoproterozoic Volta basin, Ghana. *In: Precambrian Research, 176* (1–4), 65–76. https://doi.org/10.1016/j.precamres.2009.10.004

Kent C. Condie. (1997). *Plate Tectonics and Crustal Evolution (Fourth Edition)*. Great Britain. Butterworth–Heinemann. https://doi.org/10.1016/B978–0–7506–3386–4.X5000–9

Khain, V. E. (1950). *Geotectonic development of the south–eastern Caucasus.*

Khain, V. E. (1994). *Geology of the Northern Eurasia (USSR). Second Part of the Geology of the USSR. Phanerozoic Fold Belts and Young Platforms.* Gebru¨der Borntraeger, Berlin.

Le Maitre, R. W., Streckeisen, A., Zanettin, B., Le Bas, M. J., Bonin, B., Bateman … Woolley, A. R. (2002). *Igneous Rocks: A Classifi cation and Glossary of Terms, Recommenda–tions of the International Union of Geological Sciences, Subcommission of the Systematics of Igneous Rocks*. Cambridge, UK: Cambridge University Press. https://doi.org/10.1017/CBO9780511535581

Le Bas, M. J., Le Maitre, R. W., Streckeisen A. & Zanettin B. (1986). A chemical classifi cation of volcanic rocks based on the total alkali–silica

diagram. *Journal of Petrology, 27,* 745–750. https://doi.org/10.1093/petrology/27.3.745

Marie–Françoise Brunet, Maxim V. Korotaev, Andrei V. Ershov & Anatoly M. Nikishin. (2003). The South Caspian Basin: a review of its evolution from subsidence modelling. *Sedimentary Geology, 156,* 119–148. https://doi.org/10.1016/S0037–0738(02)00285–3

Milanovsky, E. E. (1991). *Geology of the USSR.* Part 3 Moscow Univ. Press, Moscow.

Müller, D. & Groves, D. I. (2019). *Potassic igneous rocks and associated gold–copper mineralization* (5th ed.). Mineral Resource Reviews. Springer–Verlag Heidelberg. 10.1007/BFb0017712

P. Huntsman-Mapila, S. Ringrose, A. W. Mackay, W. S. Downey, M. Modisi, S. H. Coetzee, Jean-Jacques Tiercelin, A. B. Kampunzu & C. Vanderpost. (2006). Use of the geochemical and biological sedimentary record in establishing palaeoenvironments and climate change in the Lake Ngami basin. *NW Botswana, 148*(1), 51–64. https://doi.org/10.1016/j.quaint.2005.11.029

Roser, B. P. & Korsch, R. J. (1986). Determination of tectonic setting sandstone–mudstone suites using SiO_2 content and K_2O/Na_2O ratio. *Journal of Geology, 94*(5), 635–650.

Roser, B. P. & Korsch, R. J. (1988). Provenance signatures of sandstone–mudstone suites determined using discriminant function analysis of major–element data. *Chemical Geology, 67,* 119–139. https://doi.org/10.1016/0009–2541(88)90010–1

Rudnick, R. L. & Fountain, D. M. (1995). Nature and composition of the continental crust – a lower crustal perspective. *Reviews in Geophysics, 33,* 267–309. https://doi.org/10.1029/95RG01302

Rudnick, R. L. & Gao, S. (2003). Composition of the Continental Crust. The Crust: Treatise on Geochemistry, Elsevier–Pergamum, Oxford. http://dx.doi.org/10.1016/b0–08–043751–6/03016–4

Rustamov M. I. (2005). South Caspian Basin ‒ geodynimc events and processes. Baku: Nafta–Press.

Rustamov, M. I. (2008). *Geodynamics and magmatism of the Caspian–Caucasian segment of the Mediterranean belt in the Phanerozoic* (Abstract of science doctor thesis … on doctor science in Earth Sciences). 07.05.2008. Institute of Geology and Geophysics, Azerbaijan National Academy of Sciences, Baku.

Rustamov M. I. (2015). Main indicators of the collisional geodynamics of Zagros–Caucasian segment of Mediterranean belt. *Proceedings of the Azerbaijan National Academy of Sciences, Earth Sciences, 1,* 3–14.

Shaw, D. M. (1968). A review of K–Rb fractionation trends by covariance analysis. *Geochim. Cosmochim. Acta, 32,* 573–601. https://doi.org/10.1016/0016–7037(68)90050–1

Shikhalibeyli, E. Sh. (1967). Geological structure and history of the tectonic development of the eastern part of the Lesser Caucasus. Baku: Publishing house "Academy of Sciences" USSR.

Sugitani, K., Horiuchi, Y., Adachi, M. & Sugisaki, R. (1996). Anomalously low Al_2O_3/TiO_2 values of Archaean chertsfrom the Pilbara Block, Western Australia—possible evidence of extensive chemical weathering on the early earth. *Precambrian Res., 80,* 49–76. https://doi.org/10.1016/S0301–9268(96)00005–8

Taylor, S. R. & McLennan, S. M. (1985). The continental crust: its composition and evolution. Oxford: Blackwell. https://doi.org/10.1002/gj.3350210116

Verma, S. P. & Armstrong–Altrin, J. S. (2013). New multi–dimensional diagrams for tectonic discrimination of siliciclastic sediments and their application to Precambrian basins. *Chemical Geology, 355,* 117–133. https://doi.org/10.1016/j.chemgeo.2013.07.014

Zonenshain, L. P. & Le Pichon, X. (1986). Deep basins of the Black Sea and Caspian Sea as remnants of Mesozoic back–arc basins. *Tectonophysics, 123,* 181–211. https://doi.org/10.1016/0040–1951(86)90197–6

Ziegler, P. A., & Cavazza, W. (Eds.). (2001). Mesozoic and Cenozoic evolution of the Scythian Platform –Black–Sea – Caucasus Peri–Tethys Memoir 6: Peri–Tethyan Rift. Wrench Basins and Passive Margins. Me´m. Mus. natn. Hist. nat., Paris.

АДІЛЬ А. АЛІЄВ, ОРХАН Р. АББАСОВ

Інститут геології та геофізики Азербайджанської національної академії наук, пр. Г. Джавіда, 119, Баку, AZ1143, Азербайджан, Tel.: (+99412) 5100141, e-mail: ad_aliyev@mail.ru, ortal80@bk.ru

ДЖЕРЕЛА ЗНОСУ ТА ТЕКТОНІЧНІ УМОВИ ФОРМУВАННЯ ГОРЮЧИХ СЛАНЦІВ (СЕРЕДНІЙ ЕОЦЕН) ПІВДЕННО-СХІДНОГО ЗАНУРЕННЯ ВЕЛИКОГО КАВКАЗУ

Відповідно до хімічного складу, встановлені протоліти та геотектонічні умови формування горючих сланців середньо-еоценового віку, відібраних з поверхневих виходів і викидів грязьових вулканів південно-східного занурення Великого Кавказу. Отримані дані зіставлені з палеогеодинамічними умовами району дослідження. Хімічний склад сланців встановлений за допомогою мас-спектрометрів "S8 TIGER Series 2 WDXRF" і "Agilent 7700 Series ICP-MS", а при визначенні віку порід використовувалися мікроскопи "Loupe Zoom Paralux XTL 745" і "МБС-10" і цифрова камера "OptixCam".

Проведена нормалізація (порівняння з пост-архейськими сланцями Австралії, верхньою конти-нентальною корою і континентальною корою) у зв'язку з особливостями розподілу хімічних елементів, а також із застосуванням різних індексів і діаграм, встановлені джерела материнських магматичних порід і палеотектонічні умови їх формування. Встановлено, що базальт-андезитові утворення принесені з комплексів мафічних і проміжних джерел. Геотектонічні умови формування горючих сланців відповідають активним районам континентальної кори, а також зонам переходу від рифтогену до колізії або геодинамічним умовам первинної колізії. Отже, процес осадконакопичення, що відбувався в умовах мілководного морського басейну в зв'язку з первинною колізією між внутрішніми плитами, пов'язаний палеоцен-міоценовим басейном (північна гілка Мезотетіса в системі Крим-Великий Кавказ-Копетдаг). Особливу роль у встановленні походження кластичних матеріалів базальт-андезитового складу, відіграє юрський і крейдяний вулканізм, пов'язаний з субдукцією, встановленою на південному схилі Великого Кавказу (Тфанське і Вандамське підняття).